Contents lists available at SciVerse ScienceDirect

Free Radical Biology and Medicine

Original Contribution

NAD(P)H:quinone oxidoreductase 1 activity reduces hypertrophy in 3T3-L1 adipocytes

Emilie E. Vomhof-DeKrey [a], Matthew J. Picklo [a,b,c],*

[a] Grand Forks Human Nutrition Research Center, USDA-ARS, Grand Forks, ND 58203, USA
[b] Department of Pharmacology, Physiology & Therapeutics, University of North Dakota, Grand Forks, ND, USA
[c] Department of Chemistry, University of North Dakota, Grand Forks, ND, USA

ARTICLE INFO

ABSTRACT

The nuclear factor E2-related factor 2 (Nrf2)/Kelch-like ECH-associated protein 1 (Keap1) pathway responds to oxidative stress via control of several antioxidant defense gene expressions. Recent efforts demonstrate that Nrf2 modulates development of adiposity and adipogenesis. One of the major Nrf2-regulated proteins, NAD(P)H:quinone oxidoreductase 1 (NQO1), is implicated in the development of adipose tissue and obesity. However, little is known about in situ disposition of Nrf2, Keap1, and NQO1 during adipogenesis in isolated adipocytes. Based on literature data, we hypothesized that adipocyte differentiation would increase expression of the Nrf2/Keap1 pathway and NQO1. Using murine 3T3-L1 preadipocytes, we mapped an increase in NQO1 protein at limited clonal expansion and postmitotic growth arrest (Days 1–3) stages and a decrease in terminally differentiated (Day 8) adipocytes that lasted for several days afterward. Conversely, NQO1, Nrf2, and Keap1 mRNA expressions were all increased in differentiated adipocytes (Days 11–14), indicating a discrepancy between steady-state mRNA levels and resulting protein. Treatment of differentiated 3T3-L1 adipocytes with glycogen synthase kinase-3β (GSK-3β) inhibitor, LiCl, led to 1.9-fold increase in NQO1 protein. Sulforaphane enhanced NQO1 protein (10.5-fold) and blunted triglyceride and FABP4 accumulation. The decrement in triglyceride content was partially reversed when NQO1 activity was pharmacologically inhibited. These data demonstrate a biphasic response of Nrf2 and NQO1 during adipocyte differentiation that is regulated by Keap1- and GSK-3β-dependent mechanisms, and that hypertrophy is negatively regulated by NQO1 activity.

Published by Elsevier Inc.

Introduction

Obesity is associated with an increase in systemic oxidative stress [1,2]. Nuclear factor E2-related factor 2 (Nrf2) is a key transcription factor that responds to oxidative stress via binding to the antioxidant response elements (ARE) in the promoter of several antioxidant defense proteins, such as those involved in glutathione synthesis, NAD(P)H:quinine oxidoreductase 1 (NQO1), glutathione S-transferase (GST) isoenzymes, and heme oxygenase-1 (HO-1) [3,4]. Under basal conditions, the Kelch repeat region of Kelch-like ECH-associated protein 1 (Keap1) binds to the Neh2 domain of Nrf2, so that Nrf2 is sequestered to the cytoplasm and continually shuttled to the proteasome. Elevated reactive oxygen species, chemical inducers, or dietary factors such as sulforaphane cause modifications in cysteine residues of Keap1, allowing for disruption of Keap1 binding to Nrf2 [5–7]. This disruption permits Nrf2 to translocate to the nucleus to bind to the ARE-DNA sequence (TGAG/CNNNGC) within antioxidant gene promoters [4,8,9].

The Nrf2/Keap1 pathway is linked to the development of obesity, adipose deposition, and hepatic fat deposition in animal models [10,11]. Mechanistic studies show that the Nrf2/Keap1 pathway regulates lipid synthesis and adipocyte differentiation [12–15]. There is a discrepancy in the literature on whether a deficiency in Nrf2 impairs or enhances adipogenesis. Shin et al.

showed that Nrf2 knockout, immortalized mouse embryonic fibroblasts (MEFs) have increased adipogenesis and exhibited elevated lipid accumulation[16]. They also showed that Keap1 knockout, immortalized MEFs (with enhanced Nrf2 expression) differentiate slower with inhibited adipogenesis via the activation of the aryl hydrocarbon receptor signaling cascade [16]. Consistent with this study, proteomic analysis and microarray analysis of wild-type and Nrf2 knockout mouse liver confirm a negative regulation of lipogenesis by Nrf2 [13,15]. In contrast, Pi et al. demonstrated in Nrf2 knockdown primary MEFs, human adipocytes, and 3T3-L1 cells that adipogenesis was impaired given that lipid accumulation was reduced and adipogenic genes, such as peroxisome proliferator-activated receptor γ (PPARγ), were decreased [14]. Additionally a knockdown of Keap1 in 3T3-L1 cells led to lipid accumulation and adipogenic gene expression increase [14]. While these studies examined the functional impact of the Nrf2 pathway on adipogenesis, little data exist as to the in situ disposition of the Nrf2/Keap1 pathway and its target genes during adipocyte differentiation.

NQO1 activity may be an additional mechanism by which Nrf2 regulates adipose accretion. Nrf2 is a major regulator of nqo1 gene expression [8]. NQO1 is a cytoprotective enzyme that utilizes NADPH or NADH as a hydride donor to catalyze the two-electron reduction of quinones, quinone imines, and azo dyes [8]. NQO1 protein is present in human adipocytes [17]. Palming et al. showed that adipocytic NQO1 mRNA is higher in adipocytes than in adipose-derived stromal vascular cells and that expression positively correlates with BMI. Additionally, this study demonstrated that weight loss leads to a decrease in NQO1 mRNA content in adipose tissue [18]. NQO1$^{-/-}$ mice have several altered metabolic pathways resulting in significantly lower abdominal adipose tissue and increased NADPH concentrations in comparison to wild-type mice [19]. However, these animals have higher levels of triglycerides in liver and blood. While these studies examined NQO1 in a complex physiological system, little is known regarding the fate of NQO1 during adipocyte differentiation and hypertrophy in an isolated system. Based on the data above from human adipocytes, we tested the hypothesis that adipocyte differentiation leads to an increase in NQO1 and Nrf2. In this study, we utilized 3T3-L1 preadipocyte differentiated adipocytes to map the expression profile of the Nrf2/Keap1 pathway throughout the differentiation stages of adipocytes. In support of our hypothesis, we found that the steady-state NQO1, Nrf2, and Keap1 mRNA expression increased in terminally differentiated 3T3-L1 adipocytes. In contrast, NQO1 and Keap1 protein levels were all diminished as a result of terminal differentiation. During the early differentiation stages (Days 0–4), NQO1 protein increased between Days 1 and 3 (limited clonal expansion transitioning to postmitotic growth arrest) but by the start of terminal differentiation at Day 4, the NQO1 protein levels decreased. The NQO1 content was elevated in differentiated adipocytes by inhibition of GSK-3β by LiCl and Keap1 by sulforaphane (SFN). Additional SFN experiments demonstrated that SFN induced NQO1 expression and activity which led to a block in hypertrophy, an effect antagonized by the NQO1 inhibitor MAC220.

Materials and methods

Reagents

Fetal bovine serum (FBS) and bovine calf serum (BCS) were from Atlanta Biological (Lawrenceville, GA). Low glucose Dulbeccos modified Eagle's medium (DMEM), Hank's balanced salt solution (HBSS), trypsin, SDS-PAGE, and Nu-PAGE gels were purchased from Invitrogen (Carlsbad, CA). R-Sulforaphane was from LKT Laboratories, Inc. (St. Paul, MN). Bovine or human insulin, dexamethasone (DX), isobutylmethylxanthine (IBMX), LiCl, NaCl, and other chemicals were purchased from Sigma Aldrich (St. Louis, MO). Real-time qPCR primers were designed and purchased from IDT (Coralville, IA).

Cell culture

Mouse 3T3-L1 fibroblasts were obtained from American Type Culture Collection (ATCC; Manassas, VA). 3T3-L1 fibroblasts were grown in culture growth medium consisting of low glucose (5 mM) DMEM supplemented with 10% BCS. Cells were maintained in incubators at 37 °C in 5% CO$_2$/95% humidified air on 25 or 75 cm^2 flasks. For subculturing, every 3–4 days 70% confluent 3T3-L1 cells were washed twice with HBSS without Ca^{2+} or Mg^{2+} and then trypsinized with 0.25% trypsin, 0.53 mM ethylenediaminetetraacetic acid (EDTA) in HBSS for 3 min at room temperature (RT). Cells were resuspended at a density of 1200–3000 cells/cm^2 in 10% BCS/90% DMEM and media were replaced every 2 days. Differentiation of 3T3-L1 fibroblasts to mature adipocytes was induced with 10% FBS, 90% DMEM, 167 nM (1 μg/ml) bovine or human insulin, 0.5 mM IBMX, and 1 μM DX 2 days after 100% confluence (Day 0). After a 2-day incubation, the media were replaced with the following: 10% FBS, 90% DMEM, and 167 nM insulin. After another 2-day incubation, the media were replaced with 10% FBS/90% DMEM and after 4 more days (Day 8) the cells were fully differentiated. At various days throughout differentiation (Days 0–14) 3T3-L1 adipocytes were harvested by scraping, washed with PBS, and pelleted by centrifugation at 200g for 7 min. Mature adipocyte treatments of insulin (167 nM), LiCl (in water; 10, 20, 40 mM), and sulforaphane (SFN; in DMSO; 5, 10, 20 μM) were applied on Day 8 and then harvested 72 h later.

For triglyceride (TAG) experiments, 20 μM SFN was applied singly or continuously to differentiated adipocytes and harvested at various time points. Treatments with the NQO1 inhibitor, 6-methoxy-1,2-demethyl-3-[(4-nitrophenoxy)methyl]indole-4,7-dione (MAC220; in DMSO; 50 and 100 nM; kind gift from Dr. David Siegel and Dr. David Ross, University of Colorado, Denver, CO), $\pm$ 20 μM SFN were applied on undifferentiated and differentiated cells and then harvested at various time points.

RNA isolation and quantification by qPCR

RNA was isolated with QIAshredder spin column, RNeasy Mini Kit, and on-column DNase I treatment (Qiagen, Valencia, CA) using the QIAcube and following the manufacturer's protocols. Following elution of RNA, the quantity and quality of RNA were determined on a NanoDrop 8000 spectrophotometer (Thermo Fisher Scientific, Wilmington, DE) and RNA (40–100 ng) was converted to cDNA using the GoScript reverse transcription system kit (Promega, Madison, WI). Real-time reactions contained the following: 1X SYBRGreen Master Mix (Applied Biosystem, Inc., Carlsbad, CA), 250 nM Nrf2 (forward, 5′–CGAGATATACGCAGGAGAGGTAAGA-3′; reverse, 5′–GCTCGA-CAATGTTCTCCAGCTT-3′), 250 nM NQO1 (forward, 5′–TATCCTTCC-GAGTCATCTCTAGCA-3′; reverse, 5′–TCTGCAGCTTCCAGCTTCTTG-3′), 250 nM Keap1 (forward, 5′–CATCCACCCTAAGGTCATGGA-3′; reverse, 5′–CATCACGTGCAGGACACACTT-3′), or 250 nM 18S rRNA (forward, 5′–CGAACGTCTGCCCTATCAACTT-3′; reverse, 5′–CCGGAATCGAA CCCTGATT-3′) primers and 2.5–6.25 ng cDNA for Nrf2, NQO1, and Keap1 reactions and 39–98 pg cDNA for 18S rRNA reactions. The final volume of the reactions was 20 μl and dissociation curves confirmed a single amplification species.

Immunoblotting

Cell pellets were homogenized with cold homogenizing buffer (20 mM sodium phosphate, 1 mM DTPA, 0.05 mM BHT, and 0.5% Triton X-100, pH 7.4, with 1 mM DTT and 1% Protease Cocktail Inhibitor (Cat. No. P-8465, Sigma Aldrich, St. Louis, MO)) and sonicated at 3 bursts for 10 s each at 50% amplitude with a sonic dismembrator (Fisher Scientific, Waltham, MA). Protein determination was determined using the Bio-Rad protein dye kit (Bio-Rad, Hercules, CA) using bovine serum albumin as the standard. Homogenates were added to 2X SDS-PAGE Laemmli sample loading buffer (4% SDS, 20% glycerol, 0.12 M Tris, pH 6.8, 2 mM DTT) before heating to 95 °C for 5 min. Samples were electrophoresed (constant 180 V) using the Bio-Rad Criterion system with Invitrogen 12% Tris-glycine or NuPAGE 10% Bis Tris gels. Laemmli running buffer (2 M glycine, 14 mM SDS, 250 mM Trizma Base) was used for 12% Tris-glycine gels and 20X MOPS running buffer (Invitrogen, Cat. No. NP1000-02) was used for the NuPAGE 10% Bis Tris gels. Proteins were transferred to PVDF membrane (90 V for 90 min Tris-glycine, 60 V for 100 min Bis-Tris) using the Bio-Rad transfer system and Towbin's transfer buffer (0.1 M glycine, 12 mM Trizma Base, 20% methanol). Membrane was blocked with TBSM (25 mM Trizma base, 140 mM NaCl, 2.7 mM KCl, 5% nonfat dry milk) for 2 h at RT or overnight at 4 °C. Membranes were incubated with primary antibody either at RT for 2 h or overnight at 4 °C with shaking. Dilution of the primary was in TBSTM (TBSM, 0.2% Tween 20). Primary antibodies used were fatty acid binding protein 4 (FABP4) 1:1000 (Cat. No. 2120, Cell Signaling Technology, Danvers, MA); NQO1 1:2000 (generous gift from Dr. John Hayes, University of Dundee, Dundee, Scotland); C-terminal Nrf2 1:500 (Cat. No. sc-722, Santa Cruz Biotechnology, Santa Cruz, CA); Keap1 1:1000 (Cat. No. 4617, Cell Signaling Technology, Danvers, MA). NQO1 recombinant standard protein was provided by Dr. John Hayes, University of Dundee, Dundee, Scotland. Membranes were washed 4 times with TBST for 5 min each and rocking. The secondary antibody anti-rabbit 1:6000 (Cat. No. W401B, Promega, Madison, WI) in TBSTM was incubated at either 2 h at RT or overnight at 4 °C. Membranes were washed 2 times with TBST and 2 times with TBS for 5 min each wash. This was followed by incubation in Pierce ECL Western Blotting Substrate (Pierce, Rockford, IL) before chemiluminescent detection using a CDL camera (UVP BioImaging System, Upland, CA). Immunoblots were normalized to total protein in the lane which was determined using the Memcode Pierce Reversible Protein Stain Kit for PVDF membranes (Pierce, Rockford, IL).

3T3-L1 triglyceride extraction

Cells were washed with PBS and pelleted in 12 × 75 mm glass tubes by centrifugation at 210g for 5 min. To extract the lipids from the cell pellets, 1.0 ml of 3:2 hexane:2-propanol was added to each tube, vortexed for 30–60 s, and centrifuged at 1000g for 5 min at RT. The hexane:2-propanol supernatant was transferred to a 2-ml glass vial and then the extraction was repeated once more. The resulting protein cell pellet was dried at 65 °C for 24–48 h and then resuspended in 1 M sodium hydroxide and analyzed for protein content as described above with the Bio-Rad protein dye kit. The hexane:2-propanol lipid extraction was dried down under nitrogen and lipid was concentrated down with 8 – 100 μl hexane:2- propanol washes to the sides of the vial. Once all lipids were dried down, samples were capped with aluminum foil and Teflon tape, and stored at −80 °C till analysis of TAG content was determined on the Roche COBAS Integra 400+ (Roche Diagnostics, Indianapolis, IN).

NQO1 activity

The NQO1 activity was measured according to similar methods described by Scott et al. [20]. Briefly, cells were washed with PBS, pelleted, and lysed in lysis buffer containing 0.8% digitonin (in DMSO) and 2 mM EDTA in 25 mM Tris buffer, pH 7.4. Then, 15 μL of cell lysate was mixed with 270 μL of 100 mM potassium phosphate buffer at pH 7.4 containing 5.5 μM FAD, 220 μM NADH, 80 μM cytochrome c, 50 μM menadione, and 1 mM sodium cyanide. The reactions were performed at 25 °C in a clear-bottom 96-well plate and cytochrome c reduction ($\varepsilon = 19{,}600$ M^{-1}) was followed at 550 nm in a Molecular Devices UV/Vis spectrophotometer. Dicoumarol (100 μM), an inhibitor of NQO1, was added in a parallel reaction so that the difference in the rates of reaction in the presence and absence of dicoumarol would define NQO1 activity.
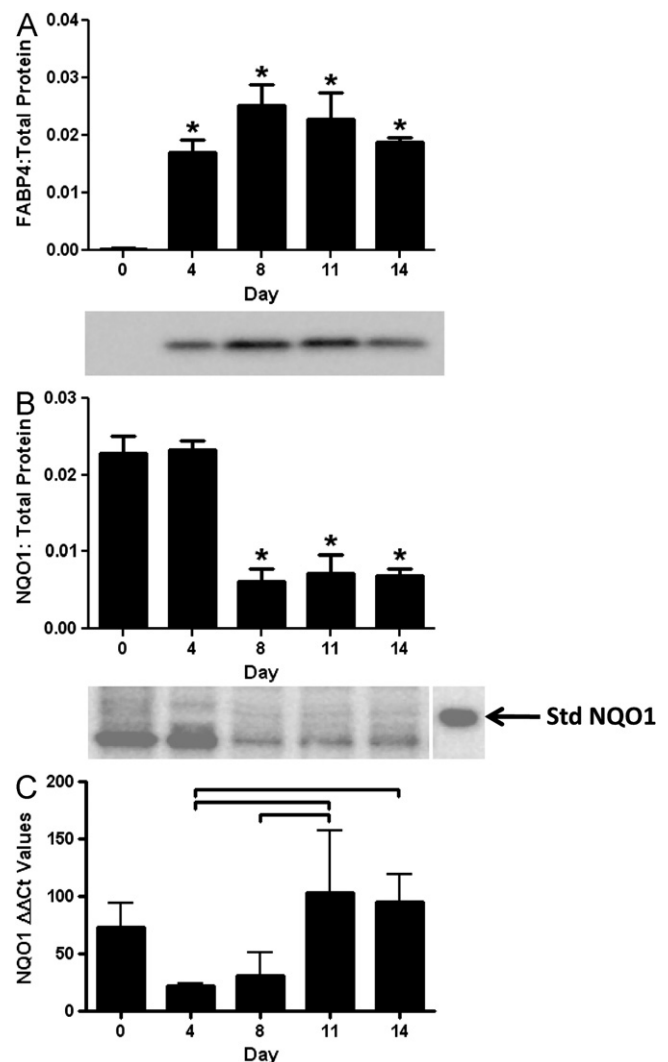

Fig. 1. NQO1 protein decreases in differentiated adipocytes while steady-state mRNA expression increases. 3T3-L1 cells were differentiated as described under Materials and methods and harvested on Days 0, 4, 8, 11, and 14. Immunoblotting of (A) FABP4 was conducted to confirm adipocyte differentiation. (B) NQO1 protein (28 kDa) expression was examined by immunoblotting and a recombinant NQO1 standard (Std) protein (32 kDa) was run alongside to confirm specificity. (C) Relative steady-state NQO1 mRNA levels were measured by SYBRGreen qPCR and normalized to 18S rRNA. Significance was determined by one-way ANOVA Dunnett's for protein and one-way ANOVA Bonferroni's for mRNA; * $P \leq 0.05$ as compared to Day 0, bars indicate $P \leq 0.05$ between samples. Data are expressed as mean ± SD; $n = 3$–4.

Statistics

All values are expressed as mean $\pm$ SD, unless otherwise noted. Statistical significance was determined by one-way ANOVA (with Dunnett's multiple comparison test or Bonferroni's multiple comparison test as appropriate) or by unpaired, two-tailed Student t test using GraphPad Prism version 5.00 for Windows (GraphPad Software, San Diego, CA, USA, www.graphpad.com). P values ≤ 0.05 were considered significant.

Results

Differentiated 3T3-L1 cells have a decrease in NQO1 and Nrf2 protein, while RNA expression increases for NQO1, Nrf2, and Keap1

Since studies with Nrf2 knockout, NQO1 knockout mice, and human obese adipose tissue demonstrate the necessity for the Nrf2/Keap1 pathway in adipogenesis, it is imperative to understand the in situ expression profile of NQO1 and its regulators Nrf2 and Keap1 in differentiating adipocytes. Therefore, we evaluated the expression profile of NQO1, Nrf2, and Keap1 mRNA and protein in 3T3-L1 adipocytes. 3T3-L1 cells were cultured to confluency (Day 0) and treated with a differentiation cocktail mix of insulin, IBMX, and DX. The cells were harvested on Days 0, 4, 8, 11, and 14. As the 3T3-L1 cells differentiated to mature adipocytes, FABP4 protein (a marker of adipocyte differentiation [21]) was significantly elevated by Day 4, as expected, in comparison to Day 0 preadipocytes (Fig. 1A). NQO1 protein after differentiation (Days 8–14) was decreased in comparison to the basal levels observed at a Day 0 (Fig. 1B). However, the NQO1 mRNA content did not reflect these changes as it increased with terminal differentiation (Fig. 1C).

When Nrf2 protein was assessed by immunoblot, there was an immunoreactive protein signal for Nrf2 at approximately 56 kDa and a smaller immunoreactive protein signal at 40 kDa of putatively degraded or possibly an isoform of Nrf2 protein when the Santa Cruz C-terminal Nrf2 antibody (No. sc-722) was used. The content of this presumably degraded Nrf2 protein increased while full-length Nrf2 decreased in the differentiated 3T3-L1 cells (Fig. 2A, gray and black bars, respectively). However, if the total Nrf2 protein was evaluated by summing the full-length and degraded Nrf2 protein signals, the overall Nrf2 protein did not change from the preadipocytes (Day 0) to differentiated adipocytes (Days 8–14) (Fig. 2A, white bars). The 56- and 44-kDa signals that we observed using a C-terminal Nrf2 antibody are lower than the theoretical molecular weight of Nrf2 (66 kDa). We also tried the Santa Cruz N-terminal Nrf2 antibody (No. sc-13032) that gave 6–7 signals ranging from ~30 to 100 kDa and another C-terminal Nrf2 antibody from R & D Systems (No. MAB3925) that gave 20+ signals ranging from ~20 to 100+ kDa (data not shown). Some studies have detected Nrf2 as a dimer at 90–110 kDa [11,22]. We did observe this dimer in only our Day 0 undifferentiated cells (along with 6 other lower molecular weight signals), but this signal was not detected at Days 4, 8, 11, and 14 (data not shown). There are numerous papers utilizing the same two Santa Cruz C-terminal and N-terminal Nrf2 antibodies, but they do not state the observed Nrf2 molecular weight on their immunoblots [4,11,12,14,22–30]. It is unfortunate that a clear and uniform consensus has not been established in published manuscripts for the appropriate molecular weight of Nrf2 on immunoblots. Therefore, since we observed discrepancies with both the C- and the N-terminal Nrf2 antibodies, our subsequent work analyzed only the mRNA expression changes of Nrf2. The steady-state Nrf2 mRNA in the differentiating 3T3-L1 cells had a profile similar to that of the NQO1 mRNA expression,
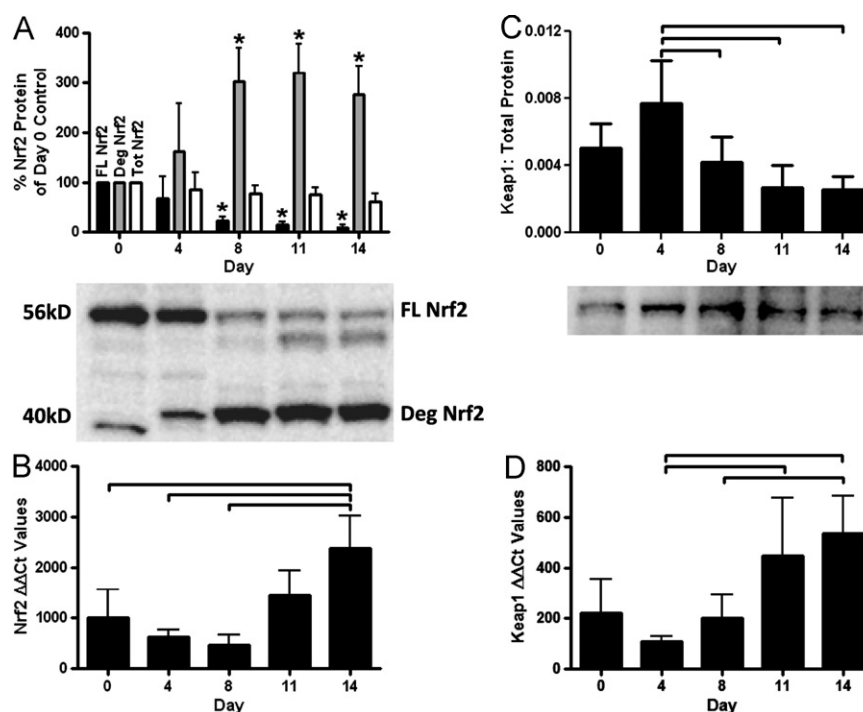

Fig. 2. Keap1 protein decreases in differentiated adipocytes, while steady-state mRNA expression for Nrf2 and Keap1 increases. 3T3-L1 cells were differentiated as described under Materials and methods and harvested on Days 0, 4, 8, 11, and 14. (A) Nrf2 and (C) Keap1 (~70 kDa) protein expression was examined by immunoblotting. Black bars, full-length (FL) Nrf2 (56 kDa); gray bars, degraded (Deg) Nrf2 (40 kDa); white bars, total (Tot) Nrf2; the sums of full-length Nrf2 and degraded Nrf2 were determined to obtain relative total Nrf2 protein expression. (B) Relative steady-state Nrf2 and (D) Keap1 mRNA levels were measured by SYBRGreen qPCR and normalized to 18S rRNA. Significance was determined by one-way ANOVA Dunnett's for protein and one-way ANOVA Bonferroni's for mRNA; * $P \leq 0.05$ as compared to Day 0, bars indicate $P \leq 0.05$ between samples. Data are expressed as mean $\pm$ SD; $n=3$–4.

where the mRNA expression was low at Day 4 and then significantly increased by Day 14 (Fig. 2B).

As a regulator of Nrf2, we assessed the expression profile of Keap1. The Keap1 protein revealed no significant change between the Day 0 and the other differentiation days, but Day 4 did have significantly more Keap1 protein than terminally differentiated 3T3-L1 cells at Days 8, 11, and 14 (Fig. 2C). The steady-state Keap1 mRNA expression also revealed a profile similar to those of NQO1 and Nrf2, in which at Day 4 the mRNA expression decreased and then by Day 14 was significantly increased (Fig. 2D).

During limited clonal expansion and postmitotic growth arrest of differentiation, NQO1 protein expression increases

Evaluations of NQO1, Nrf2, and Keap1 expression profiles have not been elucidated during the specific differentiation stages of limited clonal expansion (Days 1–2), postmitotic growth arrest (Days 3–4), and terminal differentiation of adipocytes (Days 4–8) [31–33]. Therefore, we harvested 3T3-L1 differentiating adipocytes on Days 0–4 and found that the NQO1 increased on Day 1 and peaked at Days 2 and 3 (Fig. 3A). The NQO1 protein decreased on Day 4, while Keap1 protein levels increased (Fig. 3A and D). The steady-state mRNA expression of NQO1 peaked at Days 1 and 2 (Fig. 3B), and correlated with the increase of NQO1 protein on Days 2 and 3. The content of Nrf2 mRNA was only significantly different between Day 0 and Day 2. Keap1 mRNA, however, did not correlate with the protein levels in that the

mRNA levels were decreasing in comparison to the increasing protein levels (Fig. 3D and E).

Next, we measured NQO1, Nrf2, and Keap1 expression levels more specifically from postmitotic growth arrest (Day 4) to terminal differentiation (Day 8). NQO1 and Keap1 protein levels significantly decreased directly with time (Fig. 4A and D). The mRNA content did not significantly change with time for NQO1, Nrf2, or Keap1 (Fig. 4B, C, and E). Therefore, it appears that NQO1 and Keap1 proteins are steadily being downregulated as the cells are reaching terminal differentiation into mature adipocytes, regardless of the mRNA expressions.

Restimulation of differentiated 3T3-L1 cells with insulin does not increase NQO1 protein

One explanation for the decrease in NQO1 protein could be the withdrawal of insulin during the latter stage (Day 4) of the differentiation process. Recently, Tan et al. demonstrated with the ARE-luc reporter transfected in HL-1 cardiomyocytes that the Nrf2 transcriptional activity was induced after stimulation with insulin [34]. We tested the hypothesis that stimulation of differentiated adipocytes with insulin would induce the Nrf2 activity and therefore elevate NQO1 protein. We stimulated Day 8, 3T3-L1 differentiated adipocytes with a bolus of 167 nM insulin (the concentration used for differentiation) for 72 h. However, NQO1 protein did not increase after insulin stimulation (Fig. 5).
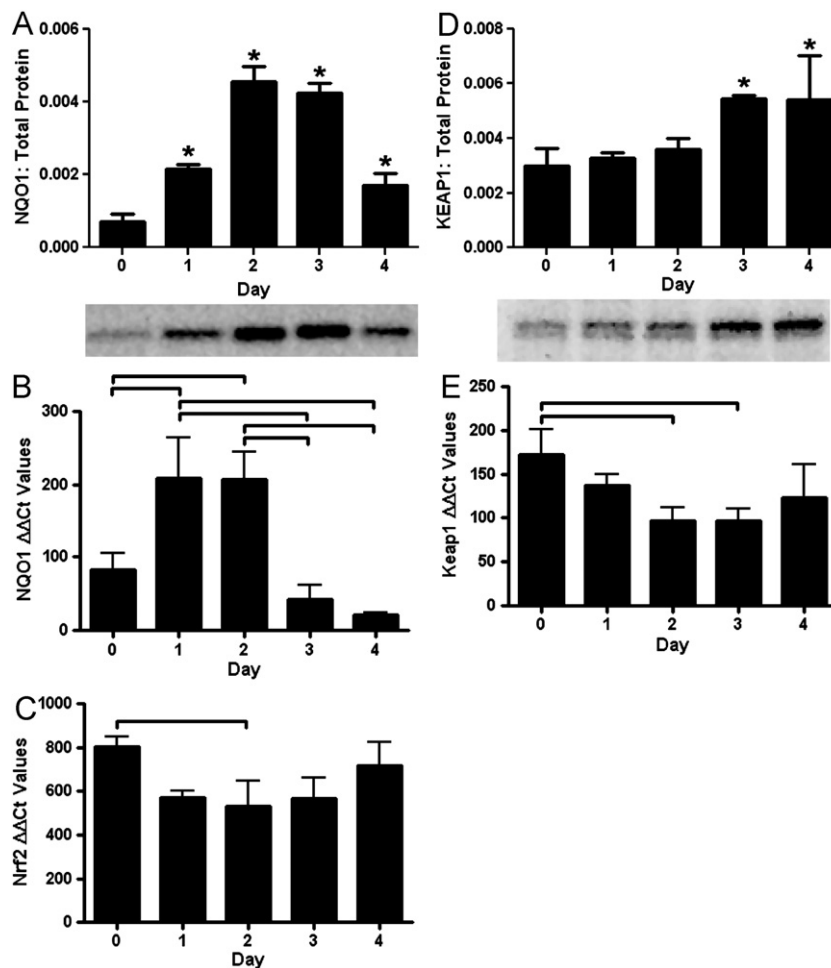

Fig. 3. NQO1 protein increases during limited clonal expansion and postmitotic growth arrest of differentiation. 3T3-L1 cells were differentiated as described under Materials and methods and harvested on Days 0, 1, 2, 3, and 4. (A) NQO1 and (D) Keap1 protein expressions were examined by immunoblotting. (B) Relative NQO1, (C) Nrf2, and (E) Keap1 mRNA levels were measured by SYBRGreen qPCR and normalized to 18S rRNA. Significance was determined by one-way ANOVA Dunnett's for protein and one-way ANOVA Bonferroni's for mRNA; * $P \leq 0.05$ as compared to Day 0, bars indicate $P \leq 0.05$ between samples. Data are expressed as mean ± SD; $n = 3$–4.
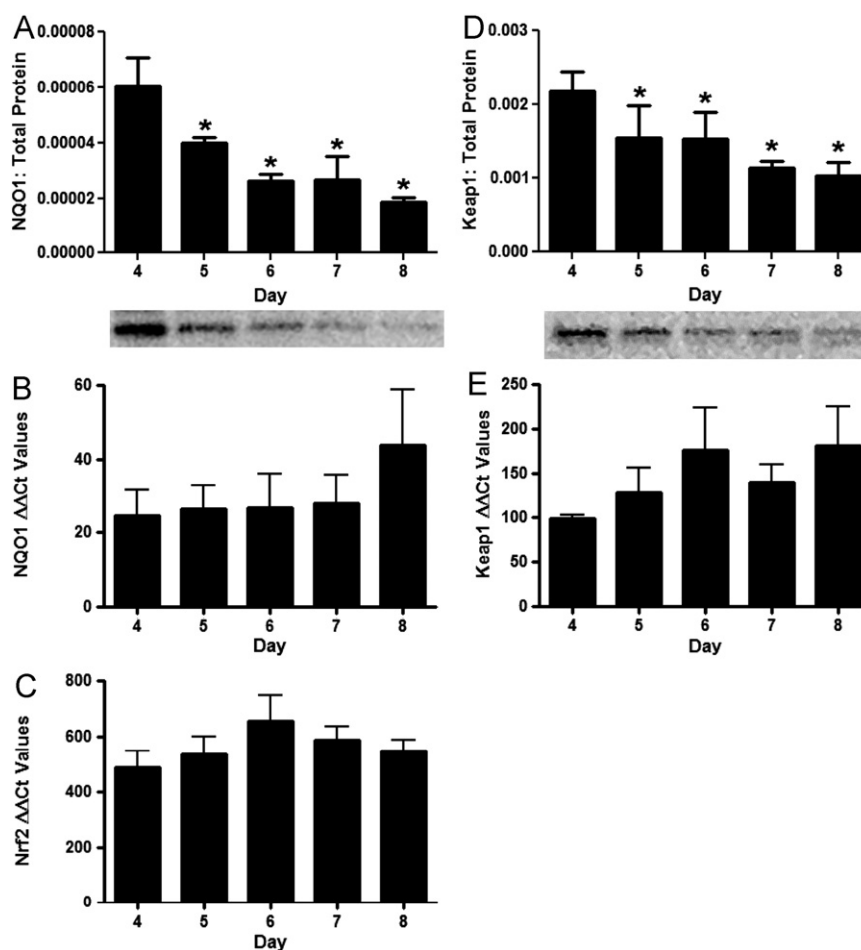
Fig. 4. NQO1 and Keap1 proteins, but not mRNA, decreases as adipocyte differentiation progresses. 3T3-L1 cells were differentiated as described under Materials and methods and harvested on Days 4, 5, 6, 7, and 8. (A) NQO1 and (D) Keap1 protein expressions were examined by immunoblotting. (B) Relative NQO1, (C) Nrf2, and (E) Keap1 mRNA levels were measured by SYBRGreen qPCR and normalized to 18S rRNA. Significance was determined by one-way ANOVA Dunnett's for protein and one-way ANOVA Bonferroni's for mRNA; * $P \leq 0.05$ as compared to Day 4. Data are expressed as mean $\pm$ SD; $n=3$.
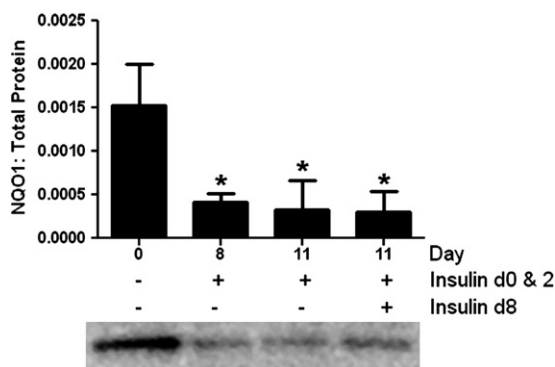

Fig. 5. Insulin restimulation does not increase NQO1 protein in differentiated adipocytes. 3T3-L1 cells were differentiated as described under Materials and methods, and then restimulated with 167 nM insulin at Day 8 (d8) and harvested on Day 11. NQO1 was examined by immunoblotting. Significance was determined by one-way ANOVA Bonferroni's; * $P \leq 0.05$ as compared to Day 0 (d0). Data are expressed as mean $\pm$ SD; $n=3$–4.

After terminal differentiation, blockade of GSK-3β and Keap1 increases NQO1

In the absence of elevated ROS, GSK-3β inhibits Nrf2 by direct phosphorylation from Fyn kinase followed by nuclear exclusion of Nrf2 [35,36]. Rojo et al. demonstrated in N2A neuroblasts that when GSK-3β was inhibited by LiCl, Nrf2 transcriptional activity increased [37]. In order to determine if GSK-3β is involved in regulating Nrf2 and NQO1 expression in differentiated 3T3-L1 adipocytes, we treated Day 8, 3T3-L1 cells with varying concentrations of LiCl and then harvested the cells 72 h later. With increasing concentrations of LiCl, NQO1 protein increased significantly over NaCl vehicle control (1.9-fold; Fig. 6A); however, there were no significant changes in NQO1 or Nrf2 message (Fig. 6B and C).

SFN is an inducer of Nrf2 signaling through interruption of the association between Keap1 and Nrf2. [7,38–41]. In order to test the hypothesis that Keap1 regulates Nrf2-dependent signaling in differentiated adipocytes, 3T3-L1 cells were treated with varying concentrations of SFN on Day 8 and harvested 72 h later. NQO1 protein and mRNA expression were significantly elevated after treatment with 20 μM SFN (10.5- and 7.6-fold, respectively; Fig. 7A and B). Conversely, evaluation of Nrf2 mRNA revealed no significant changes (Fig. 7C). These data indicate that the interaction of Keap1 with Nrf2 modulates the elevation in NQO1 expression in terminally differentiated 3T3-L1 adipocytes.

NQO1 has a mechanistic role in adipocyte hypertrophy but not differentiation

Since our data indicated that NQO1 protein was reduced in differentiated adipocytes, we tested the hypothesis that inhibition of NQO1 was requisite for adipocyte differentiation and/or hypertrophy. In order to examine this hypothesis, we used SFN to
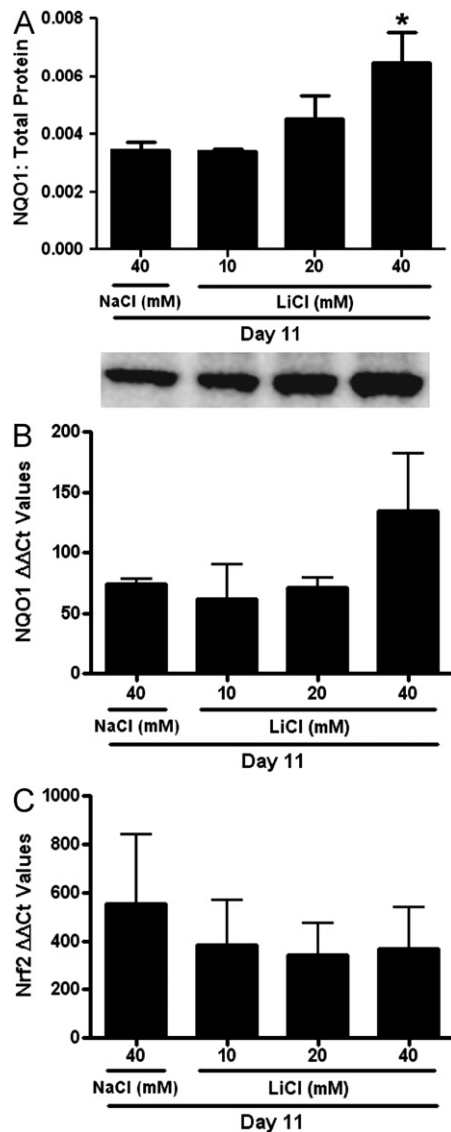
Fig. 6. LiCl treatment increases NQO1 protein, but not NQO1 mRNA. 3T3-L1 cells were differentiated as described under Materials and methods, and treated with varying concentrations of LiCl at Day 8 and harvested on Day 11. A 40 mM NaCl was used as a vehicle control (VC). (A) NQO1 was examined by immunoblotting. (B) Relative NQO1 and (C) Nrf2 mRNA levels were measured by SYBRGreen qPCR and normalized to 18S rRNA. Significance was determined by one-way ANOVA Dunnett's; * $P \leq 0.05$ as compared to VC for protein and mRNA. Data are expressed as mean ± SD; $n = 3$.

Fig. 7. Sulforaphane increases NQO1 protein and mRNA levels. 3T3-L1 cells were differentiated as described under Materials and methods, and treated with varying concentrations of sulforaphane (SFN). A 0.3% DMSO was used as a VC. (A) NQO1 was examined by immunoblotting. (B) Relative NQO1 and (C) Nrf2 mRNA levels were measured by SYBRGreen qPCR and normalized to 18S rRNA. Significance was determined by one-way ANOVA Dunnett's; * $P \leq 0.05$ as compared to VC for protein and mRNA. Data are expressed as mean ± SD; $n = 3$.

induce NQO1 expression. We reasoned that SFN, in part through inducing NQO1, would reduce adipocyte differentiation and hypertrophy.

First, we treated differentiating 3T3-L1 cells once with SFN (20 μM) on Day 4 or 7 and then harvested the cells 72 h later. In vehicle control cells, TAG content increased by Days 7 and 10 in comparison to Day 0 undifferentiated cells, an effect blunted by SFN (Fig. 8A). Second, we treated differentiating 3T3-L1 cells daily with SFN from Days 1 to 10 and harvested at Days 4, 7, and 10. In vehicle control adipocytes, TAG content increased as the 3T3-L1 cells differentiated at Days 7 and 10 in comparison to Day 0 undifferentiated cells, and the continuous treatment of SFN completely blocked the accumulation of TAG significantly in Day 7 and 10 differentiated cells (Fig. 8B). While SFN induced NQO1 protein, it inhibited the expression of FABP4 protein, an indicator of adipocyte differentiation (Fig. 8C and D).
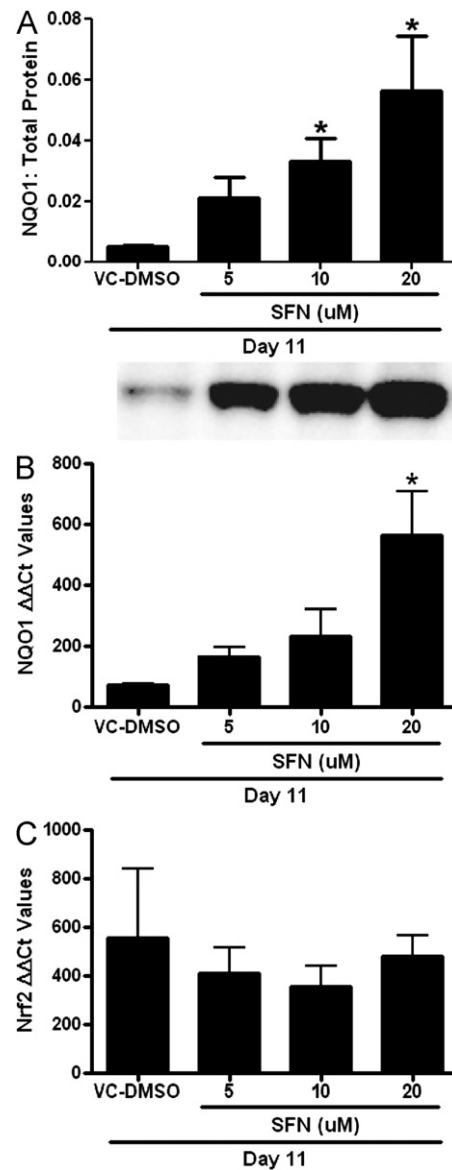
With SFN inducing the expression of NQO1 and blocking TAG accumulation, we wanted to antagonize these effects by utilizing the NQO1inhibitor MAC220. First, a time course of a single bolus of MAC220 was performed to determine how long a single dosing of MAC220 inhibited NQO1 activity. MAC220 inhibited ~70% of NQO1 activity for up to 24 h (Fig. 9A). Next, differentiating 3T3-L1 cells were treated once with SFN on Day 4 and MAC220 daily on Days 4–7 and then the cells were harvested on Day 7 (Fig. 9B). SFN alone decreased the amount of TAG content (Fig. 9C and D). However, the dual treatment of MAC220 with SFN permitted more TAG accumulation than in the cells treated only with SFN but there was still less TAG than the Day 7 untreated cells overall (Fig. 9D). This could be due to the fact that MAC220 did not completely inhibit NQO1 activity as seen in our time course data (Fig. 9A). These data indicate that adipocyte hypertrophy is negatively regulated in part by NQO1 activity.
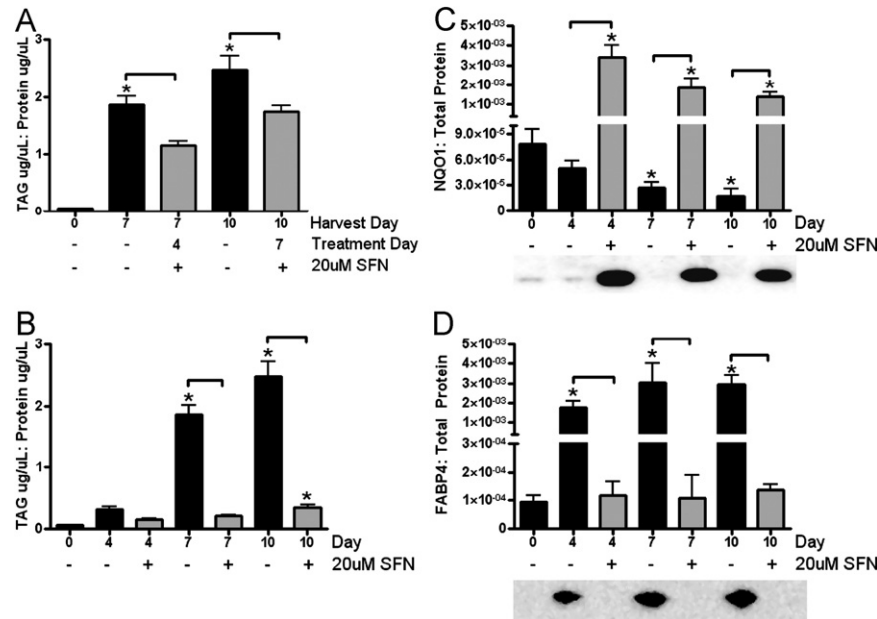
Fig. 8. Sulforaphane decreases triglyceride accumulation and blocks differentiation. 3T3-L1 cells were differentiated as described under Materials and methods, and treated with 20 μM SFN at various time points. (A) Differentiating 3T3-L1 cells were treated with SFN on Days 4 or 7, harvested 72 h later, and then TAG levels were determined. Differentiating 3T3-L1 cells were treated daily with SFN starting at Day 1 and harvested at Day 4, 7, or 10, and then (B) TAG levels, (C) NQO1 protein levels, and (D) FABP4 protein levels were determined. Significance was determined by one-way ANOVA Bonferroni's for TAG and FABP4 data and unpaired, two-tailed t test for NQO1 data; * $P \leq 0.05$ as compared to Day 0; bars indicate $P \leq 0.05$ between samples. Data are expressed as mean ± SD; $n=3$.
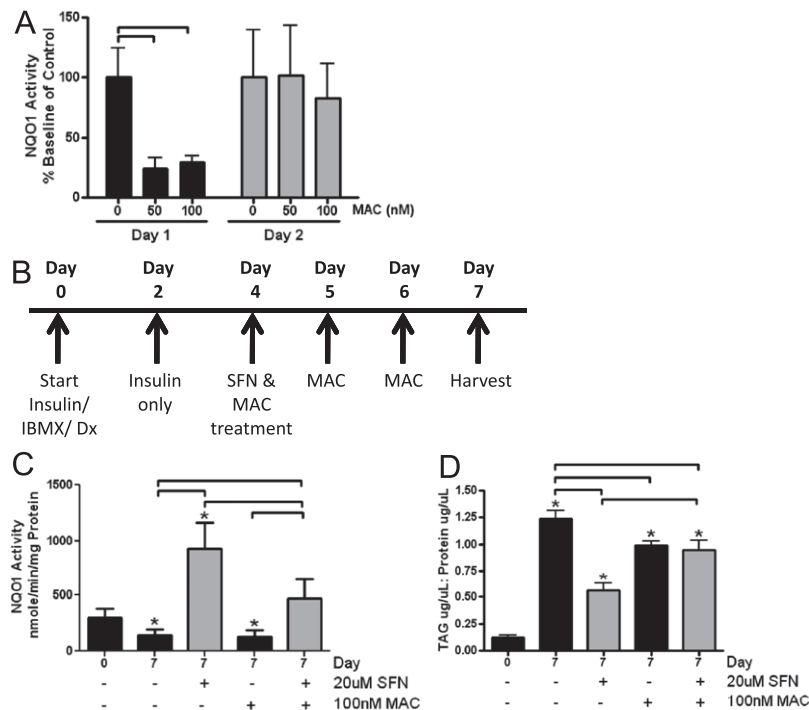

Fig. 9. Increased NQO1 activity inhibits triglyceride accumulation. 3T3-L1 cells were differentiated as described under Materials and methods, and treated with various concentrations of NQO1 inhibitor, MAC220 ± 20 μM SFN. (A) Undifferentiated 3T3-L1 cells were treated once with 50 or 100 nM MAC220 (MAC) and then harvested 24 or 48 h later in order to determine the length of MAC220 inhibition. (B) Experimental scheme in which differentiating 3T3-L1 cells were treated on Day 4 with 20 μM SFN alone, on Days 4–7 with 100 nM MAC alon, or a combination treatment of 20 μM SFN on Day 4 and 100 nM MAC on Days 4–7 and then cells were harvested on Day 7 to determine (C) NQO1 protein activity and (D) TAG content. Significance was determined by one-way ANOVA Bonferroni's for TAG data and unpaired, one-tailed t test for NQO1 activity data; * $P \leq 0.05$ as compared to Day 0; bars indicate $P \leq 0.05$ between samples. Data are expressed as mean ± SD, except MAC220 time course is as mean ± SE; $n=2$–4.

Discussion

Nrf2 and NQO1 deletion studies have implicated their necessity in adipogenesis, yet the disposition of the endogenous Nrf2/Keap1 pathway and NQO1 in differentiating adipocytes is poorly characterized. Our data demonstrate that this pathway is temporally regulated transcriptionally, perhaps translationally, and posttranslationally. NQO1 protein levels increased at Days 2 and 3 of differentiation and then diminished at Day 4. As the 3T3-L1 adipocytes became terminally differentiated (Days 5–8)

the levels of NQO1 and Keap1 protein continued to decrease. These protein levels were, however, opposite to the respective mRNA message of Nrf2, NQO1, and Keap1. SFN treatments established that the interaction of Keap1 to Nrf2 was the major regulatory mechanism controlling NQO1 protein levels instead of insulin signaling or GSK-3β pathways and that an increase in NQO1 activity by continuous SFN treatment on early differentiating 3T3-L1 cells blocked hypertrophy and differentiation.

There are contrasting data demonstrating that Nrf2 acts as either a negative or a positive regulator of adipogenesis and lipid synthesis via the utilization of Nrf2 knockout mice, Nrf2 knockdown, or Keap1 knockdown immortalized MEFs, primary MEFs, human adipocytes, or 3T3-L1 adipocytes [12,14,16]. Proteomic analyses and microarray data present Nrf2 as a negative regulator of lipid synthesis based on the number of lipid synthesis proteins and genes that are differentially regulated in the Nrf2 knockout mouse versus the wild type [13,15]. These contrasting data are similar to studies of whether ROS inhibits or enhances adipocyte differentiation [42–44].

Our data demonstrate a discrepancy between protein content and mRNA message for NQO1. These data indicate multiple levels of regulation for NQO1. We recognize that our data are limited in that the mRNA and protein levels determined are steady-state levels and do not reflect synthesis and degradation rates. Subsequent studies are needed to determine mRNA stability, translational regulation, and protein degradation parameters for NQO1 and Keap1. One possible explanation for posttranscriptional regulation of NQO1 could be through microRNA (miRNA) regulation. We found two putative miRNAs, miR-145 and miR-344b, that could bind within the mouse 3′ UTR of Nqo1 (Fig. 10). No research has been done involving miR-344b, but miR-145 and its cocistronic partner miR-143 have been studied in smooth muscle cells, subcutaneous adipose, 3T3-L1 adipocytes, and liposarcoma cell lines [45–48]. Both miR-145 and miR-143 are conserved across human, mouse, rat, chicken, zebrafish, and drosophila species [45]. Recent studies have demonstrated that their expression fluctuates during adipogenesis and that they are highly expressed in human adipose tissue. They also have roles in regulating the differentiation of smooth muscle cells [45–48]. Therefore it is conceivable that miR-145 could regulate NQO1 during adipogenesis.

Even with the NQO1 mRNA and protein regulation caveats, our data have bearing on studies examining NQO1 in the obese human condition. A study by Palming et al. demonstrated that mRNA content for NQO1 in human adipocytes is higher than stromal vascular cells isolated from subcutaneous adipose tissue [18]. This study also demonstrated that NQO1 mRNA is directly correlated with BMI and during weight loss NQO1 mRNA decreased in the subcutaneous adipose tissue [18]. Our results, however, demonstrate that NQO1 mRNA is not a surrogate for NQO1 protein. Our data, while derived from a murine adipocyte

model, clearly support the necessity to study the actual protein content of NQO1, in adipose tissue.

To elucidate the necessity of differentiating adipocytes to diminish NQO1 in order for hypertrophy to occur, we conducted various SFN and MAC220 treatments that would enhance and block NQO1 activity, respectively. SFN alone blocked TAG accumulation and was associated with an increase in NQO1 protein. In order to determine the extent to which NQO1 had a mechanistic role in blocking TAG accumulation by SFN, we used the NQO1 inhibitor MAC220. These pharmacological studies demonstrate that mechanistically NQO1 is contributing to the regulation of adipocyte hypertrophy. These studies are in seeming contrast to in vivo studies showing an increase in NQO1 with adiposity in obese people and decreases in abdominal fat in NQO1 knockout mice [18,19]. However, human obesity is associated with elevated oxidative stress, a factor not examined in this current work [18]. Secondly, adipocyte hypertrophy in the intact animal is a complex interplay of multiple interorgan signaling events and availability of lipid synthesis substrates. These parameters are likely altered in a whole animal NQO1 knockout.

In order to assess how NQO1 expression was being regulated specifically by Nrf2 during differentiation, we utilized pharmacological effectors of Nrf2. Nrf2 can be posttranslationally regulated by three primary mechanisms: insulin signaling, Keap1 binding, or GSK-3β/Fyn kinase phosphorylation [34–36,49]. In HL-1 cardiomyocytes, Nrf2 transcriptional activity was induced after insulin stimulation [34]. These data illustrate a possibility for Nrf2 activity to increase on insulin signaling in differentiated adipocytes and therefore lead to an increase in NQO1 expression. Conversely, in our terminally differentiated 3T3-L1 adipocytes, NQO1 protein expression was not changed after insulin treatment. This discrepancy could be due to the difference in cell type of HL-1 cardiomyocytes versus 3T3-L1 adipocytes.

Nrf2 activity is inhibited via phosphorylation and nuclear exclusion by the GSK-3β -Fyn kinase pathway [35,36]. On activation of the phosphatidylinositol 3-kinase (PI3K)/Akt pathway (by ROS or by insulin), GSK-3β is inhibited and Nrf2 activity is increased [28,50]. Our data show that GSK-3β inhibition with LiCl enhances NQO1 protein expression, albeit weakly, in mature adipocytes but the mRNA was not. Jain and Jaiswal demonstrated a similar result in human hepatoma HepG2 cells, in which NQO1 protein was increased, and mRNA expression was not significantly changed [36]. It is not clear, however, why insulin stimulation (see above) did not have a similar effect since insulin activates the PI3K/Akt pathway.

Keap1 negative regulation of Nrf2 takes place through direct cytosol sequestration, targeted ubiquitination by the Cullin3-containing E3-ligase complex, and shuttling of Nrf2 to the proteasome [49,51]. Utilizing the isothiocyanate, SFN, to interrupt the association of Keap1 to Nrf2, we were able to test whether Keap1 was contributing to the decrease of NQO1 protein expression in mature adipocytes through its regulation of Nrf2. Based on our data, SFN increased the NQO1 expression in 3T3-L1 adipocytes. This increase in NQO1 expression was even greater than that of the LiCl treatment. While Rojo et al. demonstrated that LiCl and SFN act additively in N2A neuroblasts, we found that addition of LiCl with SFN did not increase NQO1 protein greater than SFN alone (data not shown). These results present a model in which the lower NQO1 expression in mature adipocytes is controlled by Nrf2 sequestration in the cytoplasm by Keap1 and to a lesser extent by GSK-3β.

The production of ROS, in part through an insulin-dependent NOX4 signaling mechanism, is necessary for adipocyte differentiation [21]. The increased protein expression of NQO1 at Days 1–3 correlates temporally with ROS production during adipogenesis [44]. The level of ROS peaks between 12 and 16 h and then starts
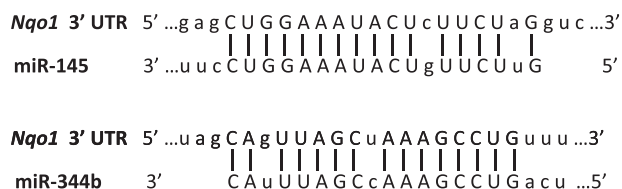
Nqo1 3′ UTR   5′ ...g a g C U G G A A A U A C U c U U C U a G g u c ...3′
                   | | | | | | | | | | | | | | | | | | |
miR-145   3′ ...u u c C U G G A A A U A C U g U U C U u G   5′

Nqo1 3′ UTR   5′ ...u a g C A g U U A G C u A A A G C C U G u u u ...3′
                   | | | | | | | | | | | | | | | | |
miR-344b   3′   C A u U U A G C c A A A G C C U G a c u ...5′

Fig. 10. Two putative miRNA binding sites in the Nqo1 3′ UTR. Sequence complementary of putative miR-145 and miR-344b binding sites in the mouse Nqo1 3′ UTR. Nqo1 NCBI mRNA reference sequence number used was NM_008706.5. Nqo1 3′ UTR was determined using the UTR database (www.utrdb.ba.itb.crnr.it) and the miRBase database (www.mirbase.org) was used to determine potential miRNA binding sites in the Nqo1 3′ UTR.

to decrease by 24 h of adipogenesis [44]. Comparatively, when NQO1 decreased at Day 4, Keap1 protein expression paralleled this decrease by increasing its protein expression at Days 3–4, indicating an indirect regulation of NQO1 by Keap1 through Nrf2. Our data mapping Nrf2 mRNA and Keap1 and NQO1 mRNA and protein levels clarify mechanisms operating during adipocyte differentiation.

Oxidative stress, ROS generation, and regulation of antioxidant defense proteins are linked to normal adipocyte function and to obesity-induced pathology. Our results support data demonstrating a decrease in glutathione S-transferase A4 in adipocytes from obese mice and a decrease in methionine sulfoxide reductase activity in visceral adipose from obese animals [52,53]. The extent to which decreases in antioxidant proteins are occurring as a result of pathological processes in adipose tissue versus resulting from the natural differentiation of preadipocytes to adipocytes still needs more clarification. We are cognizant that obesity-induced pathology within adipose tissue is complex and involves multiple cell types. Yet, our data suggest that a decrease in Nrf2-dependent antioxidant proteins, specifically NQO1, is a programmed mechanism of adipocyte biology. Our mapping of the Nrf2, Keap1, and NQO1 expression profiles suggests a tightly controlled rheostat of this pathway.

Acknowledgments

References

[1] Furukawa, S.; Tujita, T.; Shimabukuro, M.; Iwaki, M.; Yamada, Y.; Nakajima, Y.; Nakayama, O.; Makishima, M.; Matsuda, M.; Shimomura, I. Increase oxidative stress in obesity and its impact on metabolic syndrome. *J. Clin. Invest.* **114:**1752–1761; 2004.
[2] Matsuzawa-Nagata, N.; Takamura, Toshinari; Ando, Hitoshi; Nakamura, Seiji; Kurita, Seiichiro; Misu, Hirofumi; Ota, Tsuguhito; Yokoyama, Masayoshi; Honda, Masao; Mijamoto, Ken-ichi; Kaneko, Shuichi Increased oxidative stress precedes the onset of high-fat diet-induced insulin resistance and obesity. *Metabolism* **57:**1071–1077; 2008.
[3] Kaspar, J. W.; Niture, Suryakant K.; Jaiswal, Anil K Nrf2:INrf2 (Keap1) signaling in oxidative stress. *Free Radic. Biol. Med.* **47:**1304–1309; 2009.
[4] Nioi, P.; McMahon, Michael; Itoh, Ken; Yamamoto, Masayuki; Hayes, John D Identification of a novel Nrf2-regulated antioxidant response element (ARE) in the mouse NAD(P)H:quinone oxidoreductase 1 gene: reassessment of the ARE consensus sequence. *Biochem. J.* **374:**337–348; 2003.
[5] Dinkova-Kostova, A. T.; Holtzclaw, W.; David, Cole; Robert, N.; Itoh, Ken; Wakabayashi, Nobunao; Katoh, Yasutake; Yamamoto, Masayuki; Talalay, Paul Direct evidence that sulfhydryl groups of Keap1 are the sensors regulating induction of phase 2 enzymes that protect against carcinogens and oxidants. *Proc. Natl. Acad. Sci. USA* **99:**11908–11913; 2002.
[6] Eggler, A. L.; Guowen, Liu; Pezzuto, John M.; van Breemen, Richard B.; Mesecar, Andrew D Modifying specific cysteines of the electrophile-sensing human Keap1 protein is insufficient to disrupt binding to the Nrf2 domain Neh2. *Proc. Natl. Acad. Sci. USA* **102:**10070–10075; 2005.
[7] Higgins, L. G.; Kelleher, Michael O.; Eggleston, Ian M.; Itoh, Ken; Yamamoto, Masayuki; Hayes, John D Transcription factor Nrf2 mediates an adaptive response to sulforaphane that protects fibroblasts in vitro against the cytotoxic effects of electrophiles, peroxides and redox-cycling agents. *Toxicol. Appl. Pharmacol* **237:**267–280; 2009.
[8] Dinkova-Kostova, A. T.; Talalay, Paul NAD(P)H:quinone acceptor oxidoreductase 1 (NQO1), a multifunctional antioxidant enzyme and exceptionally versatile cytoprotector. *Arch. Biochem. Biophys.* **501:**116–123; 2010.
[9] Holtzclaw, W. D.; Dinkova-Kostova, Albena T.; Talalay, Paul Protection against electrophile and oxidative stress by induction of phase 2 genes: the quest for the elusive sensor that responds to inducers. *Adv. Enzyme Regul* **44:**335–367; 2004.
[10] Tanaka, Y.; Aleksunes, Lauren M.; Yeager, Ronnie L.; Gyamfi, Maxwell A.; Esterly, Noriko; Guo, Grace L.; Klaassen, Curtis D NF-E2-related factor 2 inhibits lipid accumulation and oxidative stress in mice fed a high-fat diet. *J. Pharmacol. Exp. Ther.* **325:**655–664; 2008.
[11] Zhang, Y. -K. J.; eager, Ronnie L.; Tanaka, Yuji; Klaassen, Curtis D YEnhanced expression of Nrf2 in mice attenuates the fatty liver produced by a methionine- and choline-deficient diet. *Toxicol. Appl. Pharmacol.* **245:**326–334; 2010.
[12] Huang, J.; Tabbi-Anneni, Imene; Gunda, Viswanath; Wang, Li Transcription factor Nrf2 regulates SHP and lipogenic gene expression in hepatic lipid metabolism. *Am. J Physiol. Gastrointest. Liver Physiol.* **299:**G1211–G1221; 2010.
[13] Kitteringham, N. R.; Abdullah, Azman; Walsh, Joanne; Randle, Laura; Jenkins, Rosalind E.; Sison, Rowena; Goldring, Christopher E. P.; Powell, Helen; Sanderson, Christopher; Williams, Samantha; Higgins, Larry; Yamamoto, Masayuki; Hayes, John; Park, B. Kevin Proteomic analysis of Nrf2 deficient transgenic mice reveals cellular defence and lipid metabolism as primary Nrf2-dependent pathways in the liver. *J. Proteomics* **73:**1612–1631; 2010.
[14] Pi, J.; Leung, Laura; Xue, Peng; Wang, Weiping; Hou, Yongyong; Liu, Dianzin; Yehuda-Shnaidman, Einav; Lee, Candy; Lau, Jackie; Kurtz, Theodore W.; Chan, Jefferson Y Deficiency in the nuclear factor E2-related factor-2 transcription factor results in impaired adipogenesis and protects against diet-induced obesity. *J. Biol. Chem.* **285:**9292–9300; 2010.
[15] Wu, K. C.; Cui, Julia; Yue, Klaassen; Curtis, D. Beneficial role of Nrf2 in regulating NADPH generation and consumption. *Toxicol. Sci.* ; 2011 http://dx.doi.org/10.1093/toxsci/kfr183 2011.
[16] Shin, S.; Wakabayashi, Nobunao; Misra, Vikas; Biswal, Shyam; Lee, Gum Hwa; Agoston, Elin S.; Yamamoto, Masayuki; Kensler, Thomas W NRF2 modulates aryl hydrocarbon receptor signaling: influence on adipogenesis. *Mol. Cell. Biol.* **27:**7188–7197; 2007.
[17] Siegel, D.; Franklin, Wilbur A.; Ross, David Immunohistochemical detection of NAD(P)H:quinone oxidoreductase in human lung and lung tumors. *Clin. Cancer Res.* **4:**2065–2070; 1998.
[18] Palming, J.; Sjöholm, Kajsa; Jernås, Margareta; Lystig, Theodore C.; Gummesson, Anders; Romeo, Stefano; Löhn, Lars; Löhn, Malin; Carlsson, Björn; Carlsson, Lena M. S The expression of NAD(P)H:quinone oxidoreductase 1 is high in human adipose tissue, reduced by weight loss, and correlates with adiposity, insulin sensitivity, and markers of liver dysfunction. *J. Clin. Endocrinol. Metab.* **92:**2346–2352; 2007.
[19] Gaikwad, A.; Long II, Delwin J.; Stringer, Janet L.; Jaiswal, Anil K In vivo role of NAD(P)H:quinone oxidoreductase 1 (NQO1) in the regulation of intracellular redox state and accumulation of abdominal adipose tissue. *J. Biol. Chem* **276:**22559–22564; 2001.
[20] Scott, K. A.; Barnes, J.; Whitehead, R. C.; Stratford, I. J.; Nolan, K. A. Inhibitors of NQO1: identification of compounds more potent than dicoumarol without associated off-target effects. *Biochem. Pharmacol.* **81:**355–363; 2011.
[21] Schröder, K.; Wandzioch, Katalin; Helmcke, Ina; Brandes, Ralf P Nox4 acts as a switch between differentiation and proliferation in preadipocytes. *Arterioscler. Thromb. Vasc. Biol.* **29:**239–245; 2009.
[22] Hou, Y.; Xue, P.; Bai, Y.; Liu, D.; Woods, C. G.; Yarborough, K.; Fu, J.; Zhang, Q.; Sun, G.; Collins, S.; Chan, J. Y.; Yamamoto, M.; Andersen, M. E.; Pi, J Nuclear factor erythroid-derived factor 2-related factor 2 regulates transcription of CCAAT/enhancer-binding protein I² during adipogenesis. *Free Radic. Biol. Med.* ; 2011.
[23] Cullinan, S. B.; Zhang, D.; Hannink, M.; Arvisais, E.; Kaufman, R. J.; Diehl, J. A. Nrf2 is a direct PERK substrate and effector of PERK-dependent cell survival. *Mol. Cell. Biol.* **23:**7198–7209; 2003.
[24] Faraonio, R.; Vergara, P.; Di Marzo, D.; Pierantoni, M. G.; Napolitano, M.; Russo, T.; Cimino, F. p53 suppresses the Nrf2-dependent transcription of antioxidant response genes. *J. Biol. Chem.* **281:**39776–39784; 2006.
[25] Langston, W.; Circu, M. L.; Aw, T. Y. Insulin stimulation of gamma-glutamyl-cysteine ligase catalytic subunit expression increases endothelial GSH during oxidative stress: influence of low glucose. *Free Radic. Biol. Med.* **45:**1591–1599; 2008.
[26] Maruyama, A.; Nishikawa, K.; Kawatani, Y.; Mimura, J.; Hosoya, T.; Harada, N.; Yamamato, M.; Itoh, K. The novel Nrf2-interacting factor KAP1 regulates susceptibility to oxidative stress by promoting the Nrf2-mediated cytoprotective response. *Biochem. J.* **436:**387–397; 2011.
[27] Piantadosi, C. A.; Carraway, Martha Sue; Babiker, Abdelwahid; Suliman, Hagir, B. Heme oxygenase-1 regulates cardiac mitochondrial biogenesis via Nrf2-mediated transcriptional control of nuclear respiratory factor-1. *Cir. Res* **103:**1232–1240; 2008.
[28] Wang, L.; Chen, Yan; Sternberg, Paul; Cai, Jiyang Essential roles of the PI3 kinase/Akt pathway in regulating Nrf2-dependent antioxidant functions in the RPE. *Invest. Ophthalmol. Vis. Sci.* **49:**1671–1678; 2008.
[29] Zhu, L.; Liu, Zhongbo; Feng, Zhihui; Hao, Jiejie; Shen, Weili; Li, Xuesen; Sun, Lijuan; Sharman, Edward; Wang, Ying; Wertz, Karin; Weber, Peter; Shi, Xianglin; Liu, Jiankang Hydroxytyrosol protects against oxidative damage by simultaneous activation of mitochondrial biogenesis and phase II detoxifying enzyme systems in retinal pigment epithelial cells. *J. Nutr. Biochem.* **1:**1089–1098; 2010.
[30] Kay, H. Y.; Kim, Won Dong; Hwang, Se Jin; Choi, Hueng-Sik; Gilroy, Richard K.; Wan, Yu-Jui Yvonne; Kim, Sang Geon Nrf2 inhibits LXRα-dependent hepatic lipogenesis by competing with FXR for acetylase binding. *Antioxid. Redox Signal.* **15:**2135–2146; 2011.
[31] Gregoire, F. M.; Smas, Cynthia M.; Sul, Hei Sook Understanding adipocyte differentiation. *Physiol. Rev.* **78:**783–809; 1998.
[32] Nakae, J.; Kitamura, Tadahiro; Kitamura, Yukari; Biggs, I. I. I.; William, H.; Arden, Karen, C.; Accili, Domenico The forkhead transcription factor Foxo1 regulates adipocyte differentiation. *Dev. Cell.* **4:**119–129; 2003.
[33] Lefterova, M.; Lazar, I.; Mitchell, A. New developments in adipogenesis. *Trends Endocrinol. Metab.* **20:**107–114; 2009.

[34] Tan, Y.; Ichikawa, Tomonaga; Li, Jinqing; Si, Qiusheng; Yang, Huaitao; Chen, Xiangbai; Goldblatt, Curtis S.; Meyer, Colin J.; Li, Xiaokun; Cai, Lu; Cui, Taixing Diabetic downregulation of Nrf2 activity via ERK contributes to oxidative stress-induced insulin resistance in cardia cells in vitro and in vivo. *Diabetes* **60:**625–633; 2011.

[35] Salazar, M.; Rojo, Ana I.; Velasco, Diego; de Sagarra, Rosa María; Cuadrado, Antonio Glycogen synthase kinase-3β inhibits the xenobiotic and antioxidant cell response by direct phosphorylation and nuclear exclusion of the transcription factor Nrf2. *J. Biol. Chem* **281:**14841–14851; 2006.

[36] Jain, A. K.; Jaiswal, Anil K. GSK-3β acts upstream of Fyn kinase in regulation of nuclear export and degradation of NF-E2 related factor 2. *J. Biol. Chem.* **282:**16502–16510; 2007.

[37] Rojo, A. I.; Rada, Patricia; Egea, Javier; Rosa, Angelo O.; López, Manuela G.; Cuadrado, Antonio Functional interference between glycogen synthase kinase-3 beta and the transcription factor Nrf2 in protection against kainate-induced hippocampal cell death. *Mol. Cell. Neurosci.* **39:**125–132; 2008.

[38] Angeloni, C.; Leoncini, Emanuela; Malaguti, Marco; Angelini, Sabrina; Hrelia, Patrizia; Hrelia, Silvana Modulation of phase ii enzymes by sulforaphane: implications for its cardioprotective potential. *J. Agric. Food Chem.* **57:**5615–5622; 2009.

[39] Guerrero-Beltrán, C. E.; Calderón-Oliver, Mariel; Pedraza-Chaverri, José; Chirino, Yolanda Irasema Protective effect of sulforaphane against oxidative stress: Recent advances. *Exp. Toxicol. Pathol.* ; 2010 http://dx.doi.org/10.1016/i.etp.2010.11.005.

[40] Kim, H. -J.; Barajas, Berenice; Wang, Meiying; Nel, Andre E Nrf2 activation by sulforaphane restores the age-related decrease of TH1 immunity: role of dendritic cells. *J. Allergy Clin. Immunol.* **121:**1255–1261; 2008.

[41] Zhang, Y.; Tang, Li Discovery and development of sulforaphane as a cancer chemopreventive phytochemical. *Acta Pharmacol. Sin.* **28:**1343–1354; 2007.

[42] Carrière, A.; Fernandez, Yvette; Rigoulet, Michel; Pénicaud, Luc; Casteilla, Louis Inhibition of preadipocyte proliferation by mitochondrial reactive oxygen species. *FEBS Lett* **550:**163–167; 2003.

[43] Carrière, A.; Carmona, Maria-Carmen; Fernandez, Yvette; Rigoulet, Michel; Wenger, Roland H.; Pénicaud, Luc; Casteilla, Louis Mitochondrial reactive oxygen species control the transcription factor CHOP-10/GADD153 and adipocyte differentiation. *J. Biol. Chem.* **279:**40462–40469; 2004.

[44] Lee, H.; Lee, Yoo Jeong; Choi, Hyeonjin; Ko, Eun Hee; Kim, Jae-woo Reactive oxygen species facilitate adipocyte differentiation by accelerating mitotic clonal expansion. *J. Biol. Chem.* **284:**10601–10609; 2009.

[45] Cordes, K. R.; Sheehy, N. T.; White, M. P.; Berry, E. C.; Morton, S. U.; Muth, A. N.; Lee, T. H.; Miano, J. M.; Ivey, K. N.; Srivastava, D. miR-145 and miR-143 regulate smooth muscle cell fate and plasticity. *Nature* **460:**705–710; 2009.

[46] Ugras, S.; Brill, E.; Jacobsen, A.; Hafner, M.; Socci, N. D.; Decarolis, P. L.; Khanin, R.; O'Connor, R.; Mihailovic, A.; Taylor, B. S.; Sheridan, R.; Gimble, J. M.; Viale, A.; Crago, A.; Antonescu, C. R.; Sander, C.; Tuschl, T.; Singer, S. Small RNA sequencing and functional characterization reveals MicroRNA-143 tumor suppressor activity in liposarcoma. *Cancer Res.* **71:**5659–5669; 2011.

[47] Ortega, F. J.; Moreno-Navarrete, J. M.; Pardo, G.; Sabater, M.; Hummel, M.; Ferrer, A.; Rodriguez-Hermosa, J. I.; Ruiz, B.; Ricart, W.; Peral, B.; Fernandez-Real, J. M. MiRNA expression profile of human subcutaneous adipose and during adipocyte differentiation. *PLoS One.* *e9022* ; 2010.

[48] McGregor, R. A.; Choi, M. S. microRNAs in the regulation of adipogenesis and obesity. *Curr. Mol. Med.* **11:**304–316; 2011.

[49] Katoh, Y.; Iida, Katsuyuki; Kang, Moon-IL; Kobayashi, Akira; Mizukami, Mio; Tong, Kit I.; McMahon, Michael; Hayes, John D.; Itoh, Ken; Yamamoto, Masayuki Evolutionary conserved N-terminal domain of Nrf2 is essential for the Keap1-mediated degradation of the protein by proteasome. *Arch. Biochem. Biophys.* **433:**342–350; 2005.

[50] Woodgett, J. R. Recent advances in the protein kinase B signaling pathway. *Curr. Opin. Cell Biol.* **17:**150–157; 2005.

[51] Villeneuve, N. F.; Lau, Alexandria; Zhan, Donna D Regulation of the Nrf2-Keap1 antioxidant response by the ubiquitin proteasome system: an insight into cullin-ring ubiquitin ligases. *Antioxid. Redox Signal.* **13:**1699–1712; 2010.

[52] Grimsrud, P. A.; Picklo, Sr.; Matthew, J.; Griffin, Timothy J.; Bernlohr, David A Carbonylation of adipose proteins in obesity and insulin resistance. *Mol. Cell. Proteomics* **6:**624–637; 2007.

[53] Uthus, E. O.; Picklo, Sr.; Matthew, J. Obesity reduces methionine sulphoxide reductase activity in visceral adipose tissue. *Free Radic. Res.* **45:**1052–1060; 2011.